Supporting Information for

Exchange Coupling and Magnetic Blocking in Dilanthanide Complexes Bridged by the Multi-Electron Redox-Active Ligand 2,3,5,6-Tetra(2-pyridyl)pyrazine

Selvan Demir,[a] Michael Nippe,[a] Miguel I. Gonzalez[a] and Jeffrey R. Long*[a]

[a]*Department of Chemistry, University of California, Berkeley, California 94720, USA. Email: jrlong@berkeley.edu*

Chem. Sci.

Table of Contents

Table S1. Redox potentials[a] observed in THF (0.1 M NBu_4PF_6) for complexes **1-3**.

complex	$E^{1/2}$(red1)	$E^{1/2}$(red2)	$E^{1/2}$(red3)	$E^{1/2}$(red4)
1	-0.64	-1.37	-2.21	-2.88
2	-0.68	-1.40	-2.26	-2.94
3	-0.64	-1.36	-2.22	-2.90

[a] Potentials in V; referenced to internal ferrocene (Fc); ν = 50 mV/s.

Table S2. Crystallographic Data.

Compound	**1**·4THF	**2**·3THF	**3**·3THF	**6**·7THF
Formula	C104 H128 B Gd2 N6 O4	C100 H120 B N6 O3 Tb2	C100 H120 B Dy2 N6 O3	C110 H160 Dy2 K N8 O13
Crystal system	Triclinic	Triclinic	Triclinic	Monoclinic
Space group	*P-1*	*P-1*	*P-1*	*Cc*
a, Å	16.4717(6)	16.0950(7)	16.083(5)	22.168(3)
b, Å	17.8945(7)	17.7564(9)	17.739(5)	25.230(3)
c, Å	18.2112(7)	18.5863(9)	18.562(5)	20.706(2)
α, °	115.277(2)	115.256(2)	115.198(5)	90
β, °	98.616(2)	105.236(2)	105.294(5)	111.311(2)
γ, °	102.884(2)	103.493(2)	103.514(5)	90
V, Å^3	4545.2(3)	4256.5(4)	4243(2)	10789(2)
Z	2	2	2	4
ρ, Mg m^{-3}	1.353	1.391	1.401	1.334
R1[a], *w*R2[b] ($I > 2\sigma(I)$)	0.0423, 0.0745	0.0327, 0.0727	0.0303, 0.0688	0.0511, 0.1190
R1[a], *w*R2[b] (all data)	0.0757, 0.0850	0.0361, 0.0738	0.0389, 0.0726	0.0753, 0.1351

[a]$R1 = 3||F_o| - |F_c||/3|F_o|$. [b]$wR2 = [3[w(F_o^2 - F_c^2)^2]/3[w(F_o^2)^2]]^{½}$, $w = 1/\sigma^2(F_o^2) + (aP)^2 + bP$, where $P = [\max(0 \text{ or } F_o^2) + 2(F_c^2)]/3$.

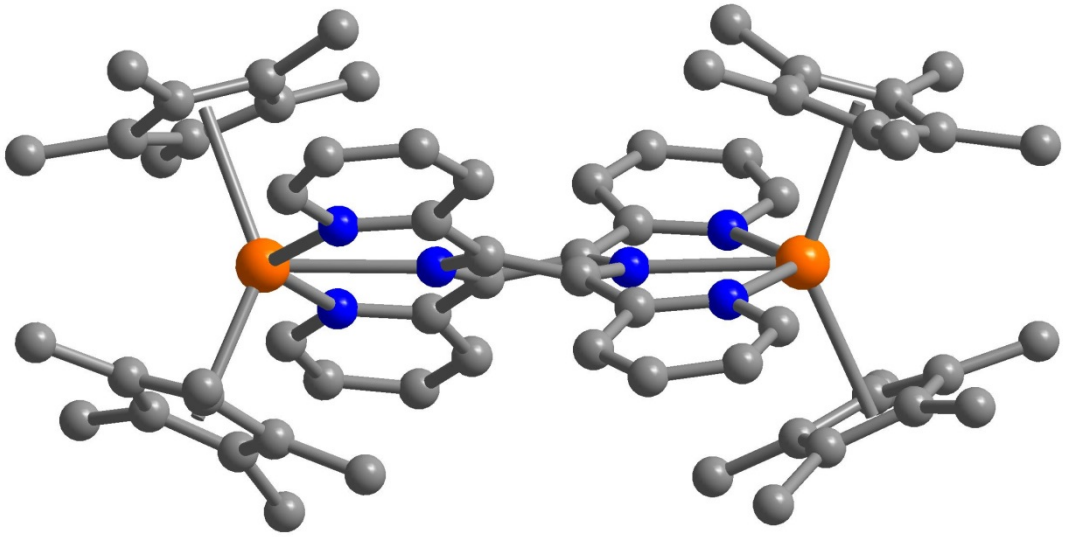

Figure S1. Structure of the $tppz^{\bullet-}$ radical-bridged cation in complex **1**. Orange, blue and gray spheres represent Gd, N and C atoms, respectively; H atoms have been omitted for clarity.

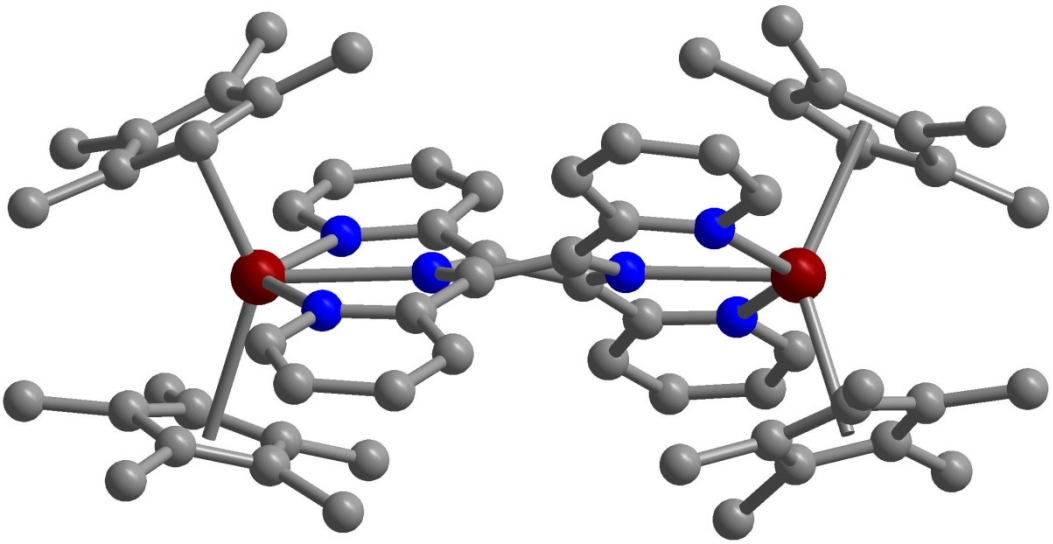

Figure S2. Structure of the tppz$^{\bullet-}$ radical-bridged cation in complex **2**. Red, blue and gray spheres represent Tb, N and C atoms, respectively; Hydrogen atoms have been omitted for clarity.

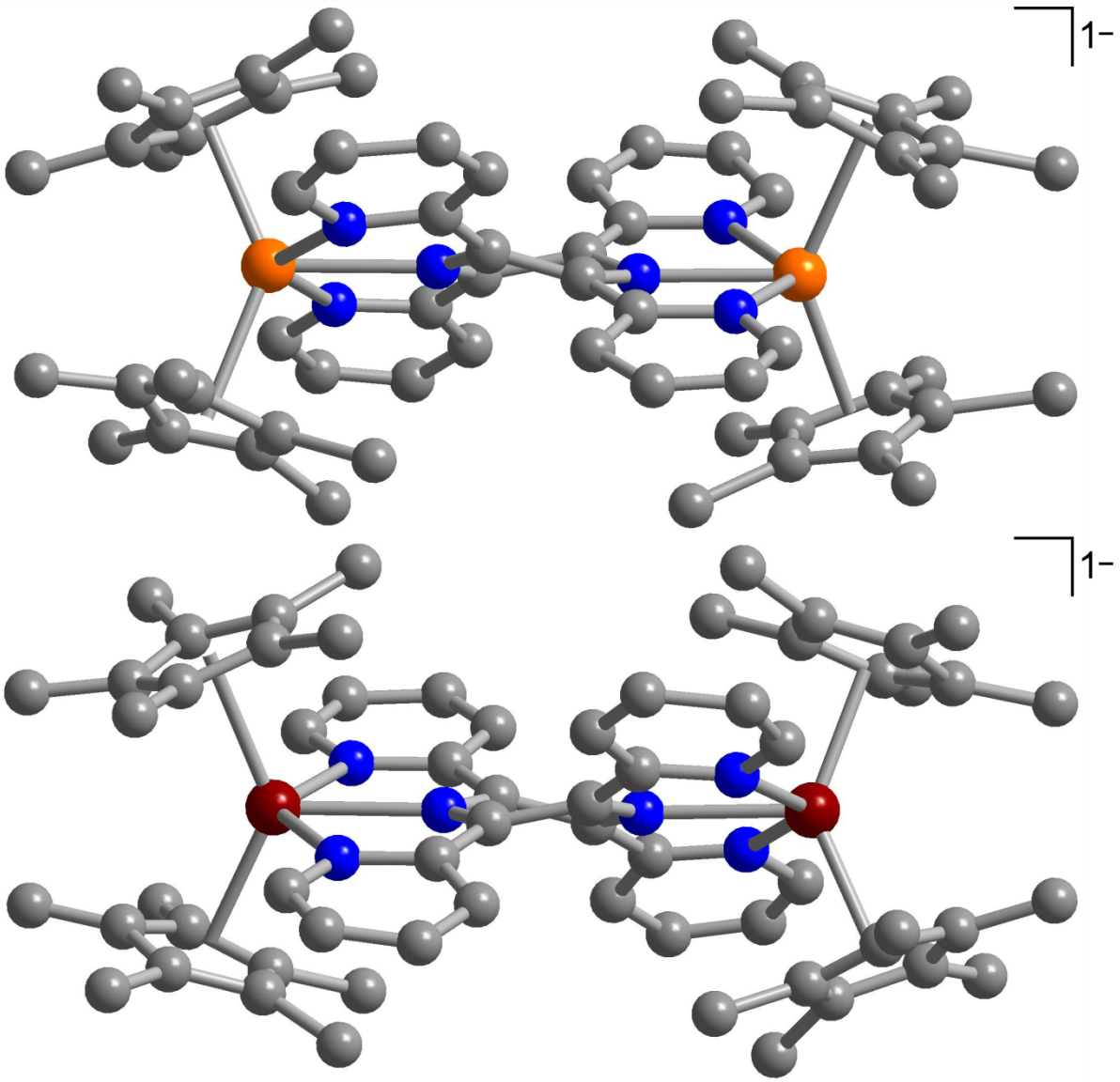

Figure S3. Top: Structure of the dinuclear monoanionic fragment in the crystal structure of **4**, showing unaltered intramolecular connectivity upon two e^- reduction of the monocation in **1**. Orange, blue and gray spheres represent Gd, N and C atoms, respectively; H atoms have been omitted for clarity. Bottom: Structure of the dinuclear monoanionic fragment in the crystal structure of **5**. Red, blue and gray spheres represent Tb, N and C atoms, respectively; H atoms have been omitted for clarity.

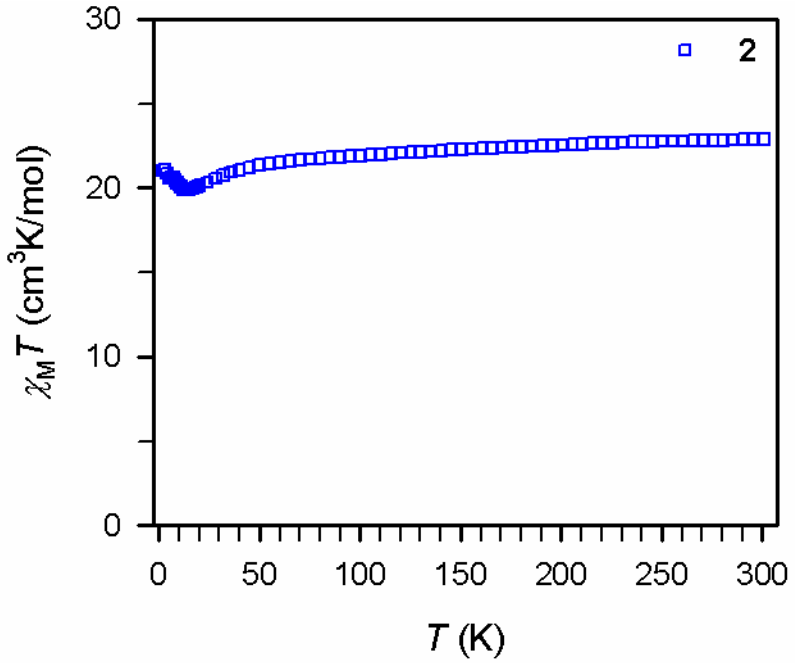

Figure S4. Variable-temperature dc magnetic susceptibility data for restrained polycrystalline samples of **2** collected under a 1 kOe applied dc field.

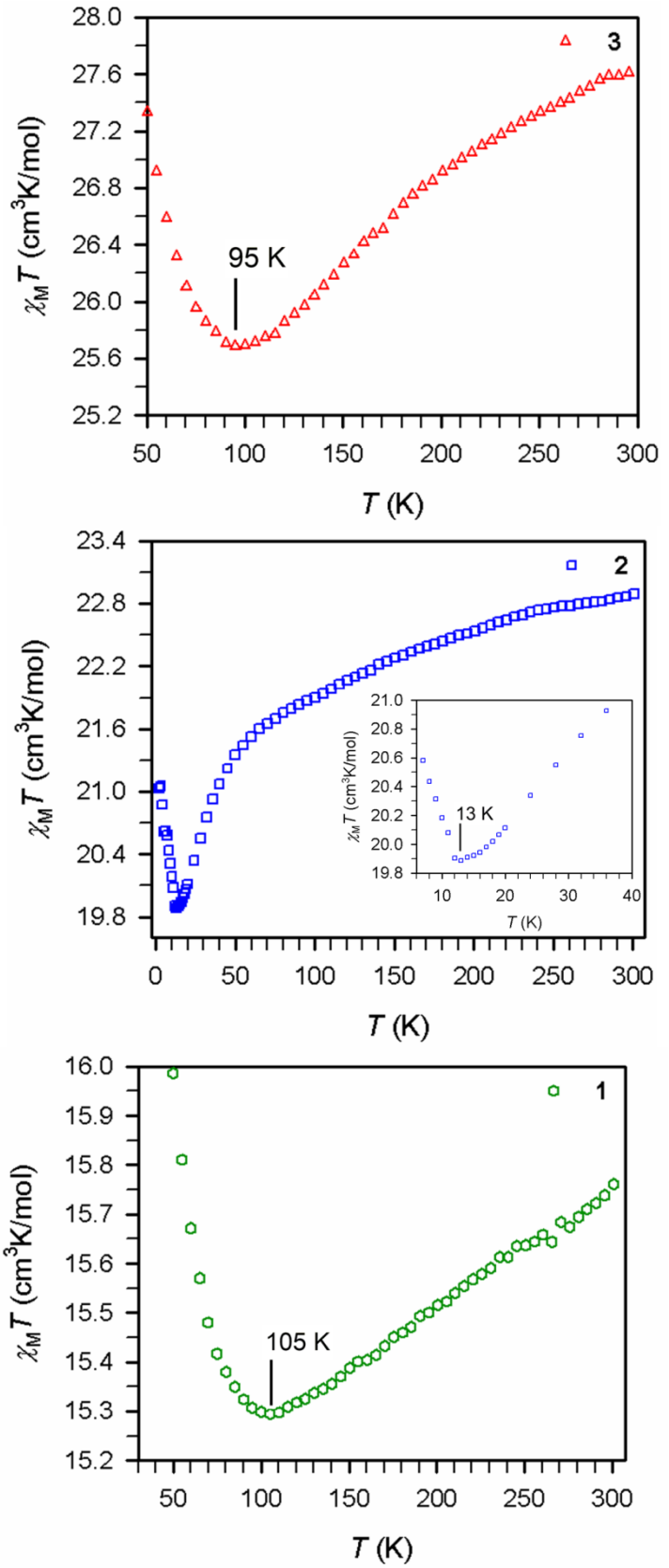

Figure S5. Variable temperature dc susceptibility data for **1** (bottom), **2** (middle), and **3** (top), zoomed in to emphasize the minima in $\chi_M T$ at high-T for each complex. Y-axis values were arbitrarily chosen for each complex in order to provide the best view of the minima for each data set.

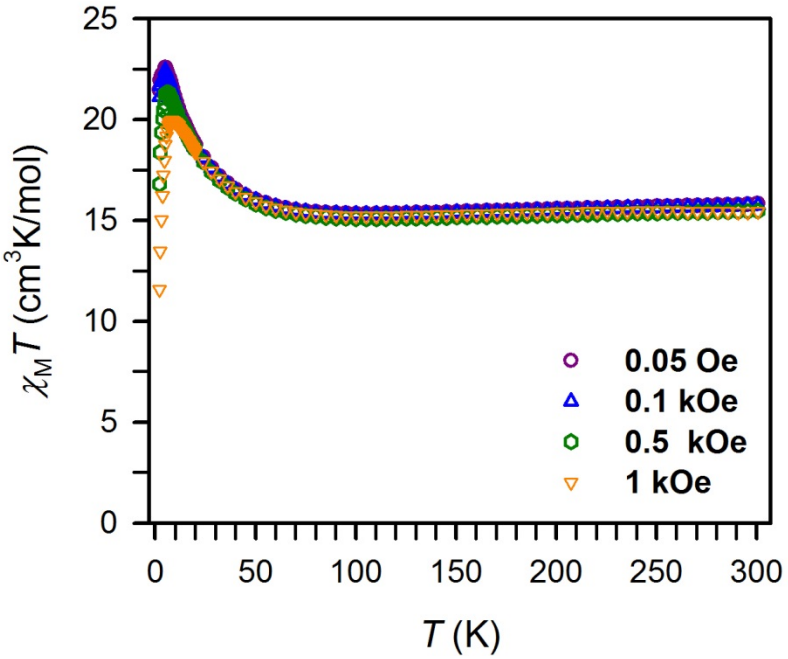

Figure S6. Variable temperature dc susceptibility data of polycrystalline **1** collected under 0.05 kOe (purple circles), 0.1 kOe (blue triangles), 0.5 kOe (green hexagons), 1 kOe (orange triangles) applied dc field.

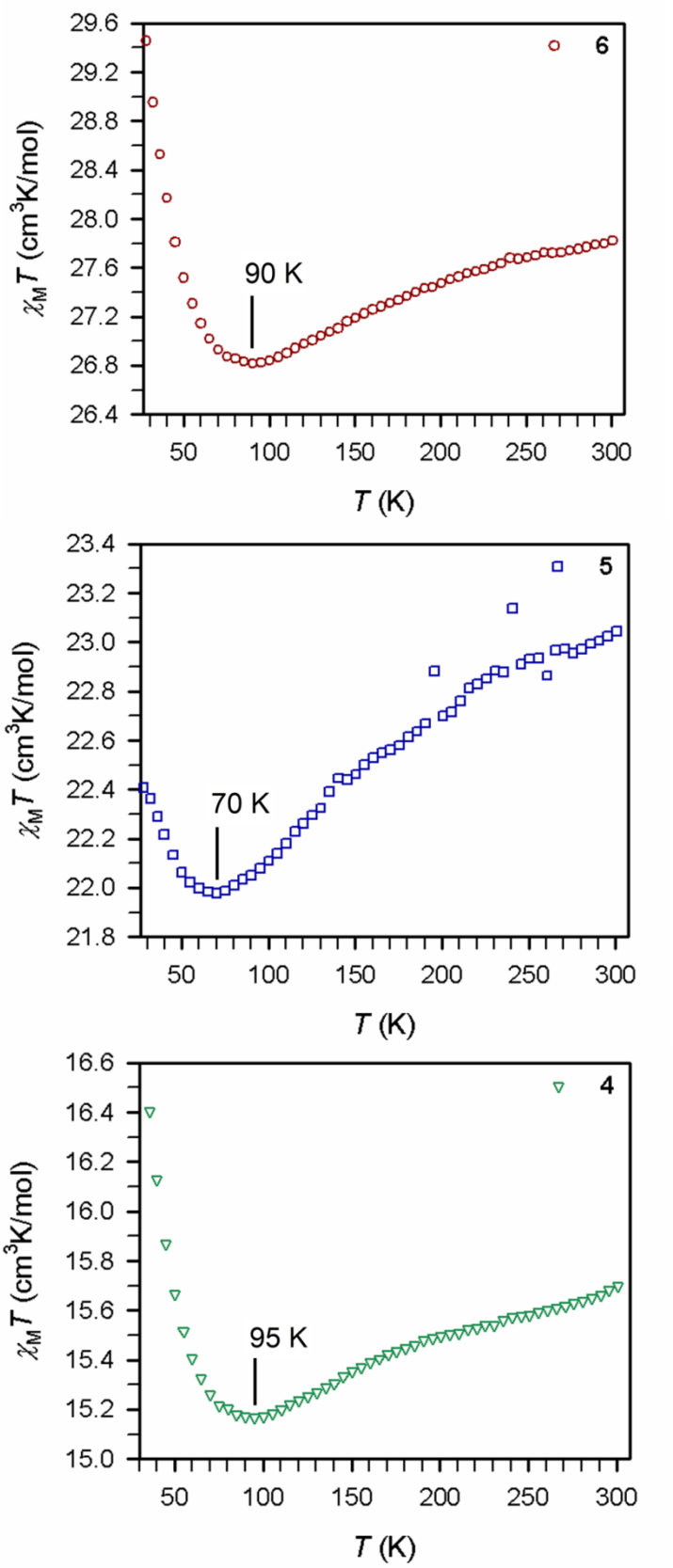

Figure S7. Variable temperature dc susceptibility data for **4** (bottom), **5** (middle), and **6** (top), zoomed in to emphasize the minima in $\chi_M T$ at high-T for each complex. Y-axis values were arbitrarily chosen for each complex in order to provide the best view of the minima for each data set.

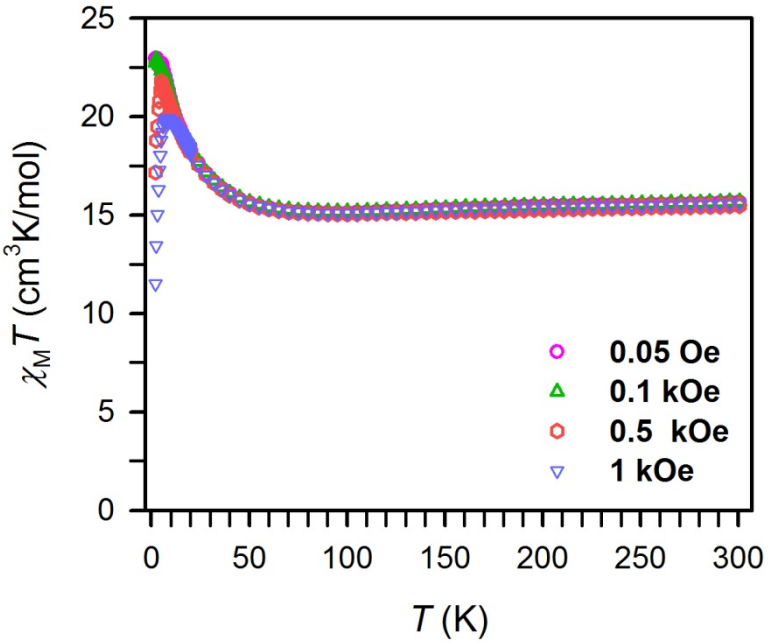

Figure S8. Variable temperature dc susceptibility data of polycrystalline **4** collected under 0.05 kOe (pink circles), 0.1 kOe (green triangles), 0.5 kOe (red hexagons), 1 kOe (blue triangles) applied dc field.

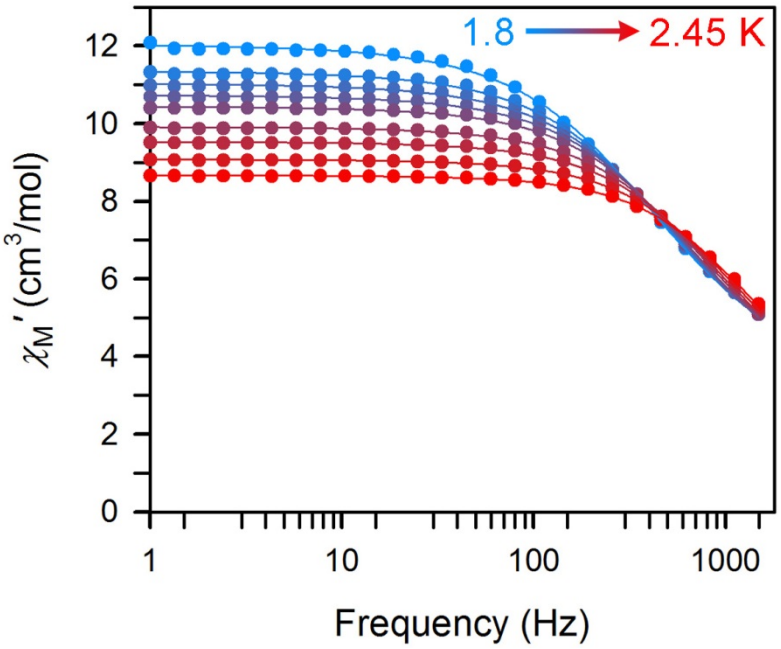

Figure S9. In-phase (χ_M', top) components of the ac magnetic susceptibility for **2** under zero applied dc field from 1.8 K (blue circles) to 2.45 K (red circles). Solid lines represent a fit to the data.

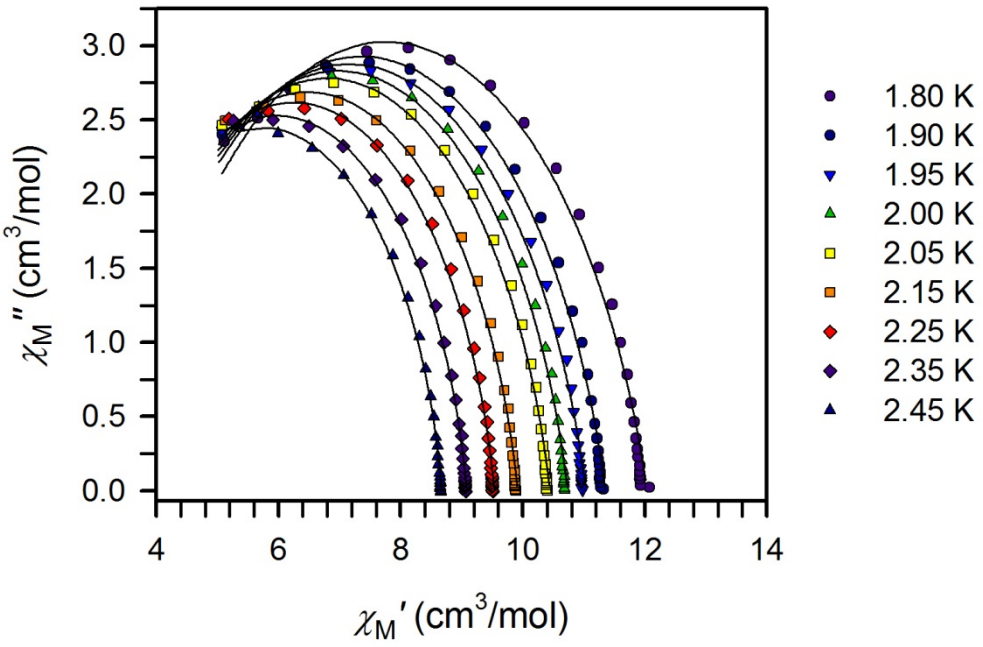

Figure S10. Cole-Cole (Argand) plots for ac susceptibility collected under zero applied dc field for **2**. Symbols represent the experimental data points and the points representing the fits are connected by solid black lines.

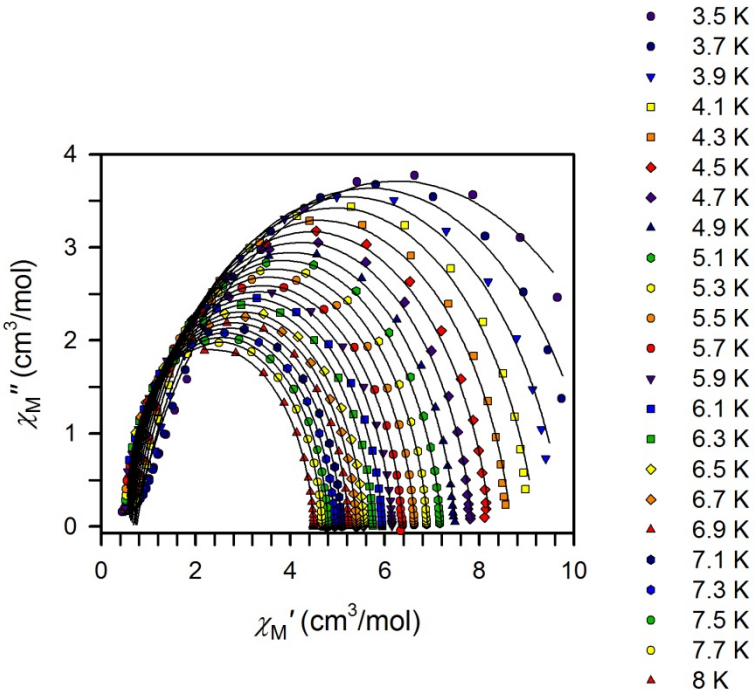

Figure S11. Cole-Cole (Argand) plots for ac susceptibility collected under zero applied dc field for **3**. Symbols represent the experimental data points and the points representing the fits are connected by black solid lines.

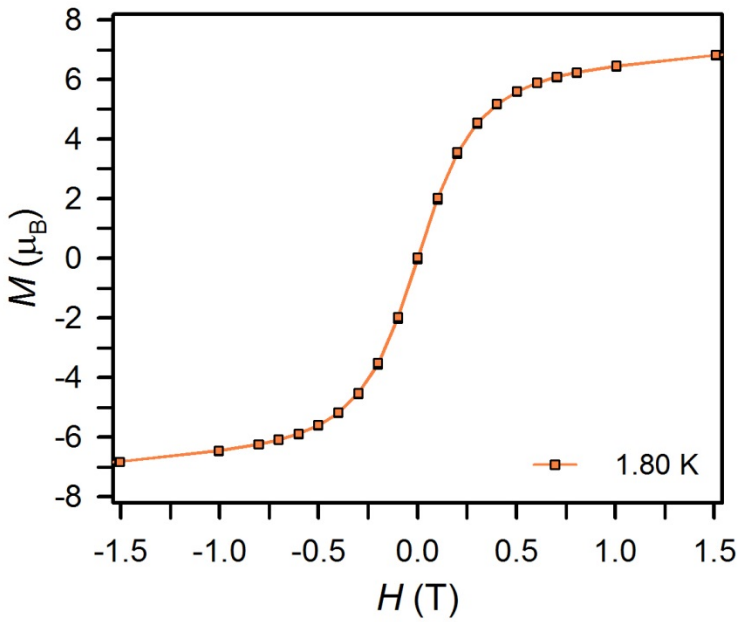

Figure S12. Variable field magnetization (*M*) data for **2** collected at 1.8 K at an average sweep rate of 0.004 Ts^{-1}.